

# Electric Potential Distribution in Modeled Human Muscle Excited by a Pulse Source

Andrijana Kuhar, *Member, IEEE*, Lidija Olooska-Gagoska, *Member, IEEE*, and Ljuben Janev

**Abstract** — The presented method determines the electric potential distribution in a modeled human muscle excited by a current pulse source placed on its surface. The electric potential in the muscle volume is calculated while considering the anisotropic and dispersive properties of its conductivity and permittivity. The developed numerical procedure is based on solving the differential equation for the electric potential in the frequency domain, by implementing the Finite Differences Method (FDM). The current density is calculated in the frequency domain using the known values for the potential. The time shape of the current pulse in different locations within the muscle tissue is analyzed using the Discrete Fourier Transform (DFT).

The application of this method includes several fields of biomedical engineering: determination of the optimal magnitude and shape of the current pulses in Electrical Muscle Stimulation (EMS), optimization of electrode shape in Transthoracic Defibrillation of the Heart, and it can be appropriately modified for usage in simulating Electromyography (EMG). The developed method can be used in every case which involves injecting electrical current on the boundary of an imperfect, dispersive, anisotropic volume conductor.

**Key words** — Current pulse source, electric potential distribution, human muscle tissue.

## I. INTRODUCTION

A SIGNIFICANT number of medical procedures implement electrical current injection in the human body, in diagnostics, as well as in therapeutic purposes. Important examples of such medical procedures are Heart Defibrillation, Electrical Muscle Stimulation and Electromyography. In those procedures determination of the current density distribution in human tissues is essential in order to achieve optimization of the injected current wave-form, amplitude and frequency. The current density can be directly determined through solving the differential equation for the electric potential in the domain of interest.

Determination of the electric potential in biological tissues is complicated due to their inhomogeneous, anisotropic and dispersive properties. As a result there are a number of papers where the anisotropic characteristics of the muscle tissue are neglected [1], [2], [3]; and works in which dispersion is neglected [1], [2], [4], [5], [6]. Our

research is focused on developing a more general technique for determination of the electric potential and current density distribution within human muscle tissue, i.e. taking into account all of the important muscle properties.

## II. MODELING THE MUSCLE TISSUE AND ELECTRODES

The muscle is modeled as a finite imperfect volume conductor with dimensions  $100 \times 100 \times 600 \text{ mm}^3$ . The geometry and dimensions of the simple muscle model are shown in Fig. 1.

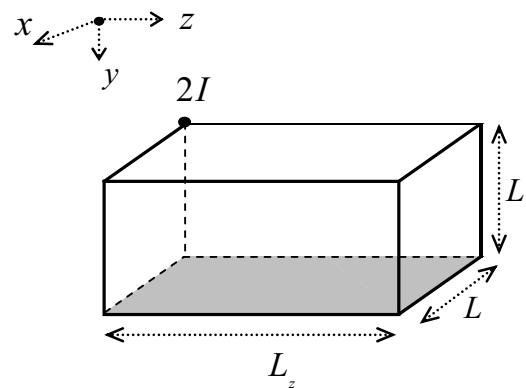


Fig. 1: The geometry of the modeled muscle volume

The symmetry of the model allows to be analyzed one quarter of the whole muscle volume, with application of appropriate boundary conditions on its borders. As shown in Fig. 1, the upper electrode is modeled as a point current source located on the upper surface of the muscle, and the grounded electrode is represented by a grounded conducting plane surface. Fig. 2 (a) shows the excitation current pulse injected by the upper electrode, and Fig. 2 (b) presents the frequency spectrum of the pulse.

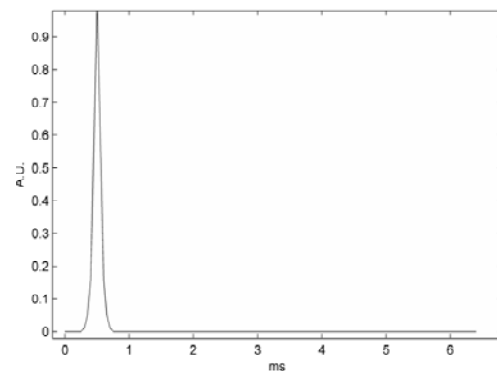


Fig. 2 (a) Time shape and duration of the excitation current pulse.

A. Kuhar, Faculty of Electrical Engineering and IT, Skopje, Republic of Macedonia (tel: +389-70-797070, e-mail: kuhar@feit.ukim.edu.mk )

L. O. Gagoska, Faculty of Electrical Engineering and IT, Skopje, Republic of Macedonia ( e-mail:lideo@feit.ukim.edu.mk )

L. Janev, Faculty of Electrical Engineering and IT, Skopje, Republic of Macedonia (e-mail: ljanev@feit.ukim.edu.mk )

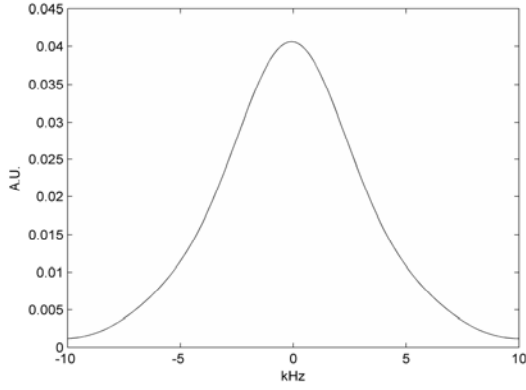


Fig. 2 (b) Frequency spectrum of the excitation current pulse.

The anisotropic properties of muscle tissue are reflected by introducing its permittivity and conductivity as tensors:  $\varepsilon = (\varepsilon_T, \varepsilon_T, \varepsilon_L)$  and  $\sigma = (\sigma_T, \sigma_T, \sigma_L)$ . According to [7], the transversal and longitudinal components of its permittivity and conductivity are dependent on frequency, as shown in Fig. 3 (a) and 3 (b).

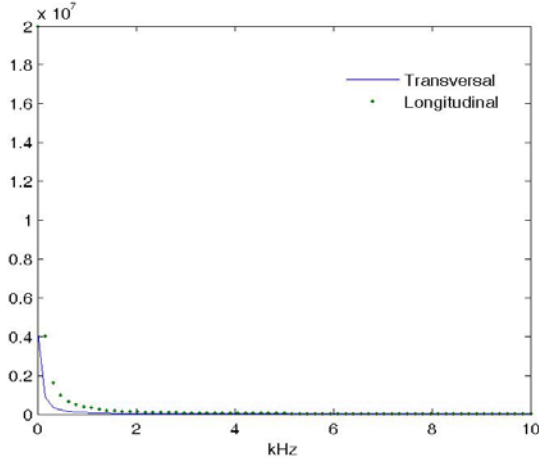


Fig. 3 (a) Permittivity of human muscle tissue as a function of frequency.

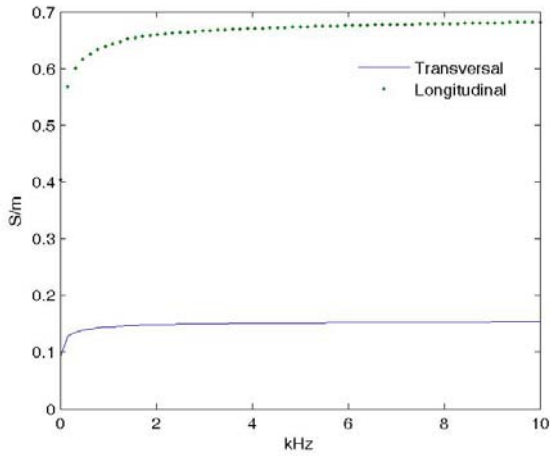


Fig. 3 (b) Conductivity of human muscle tissue as a function of frequency.

### III. NUMERICAL PROCEDURE

The developed numerical procedure is based on solving the differential equation for the electric potential by implementing the Finite Differences Method [8]. In order to implement FDM on the imperfect conductor, its volume is divided into  $N = N_x \cdot N_y \cdot N_z$  three dimensional elements. According to FDM, the end points of the cubic shaped elements are called nodes. The point current source is represented by a node located in the origin of the coordinate system.

The differential equation for the electrostatic potential is obtained by combining Maxwell's first equation in complex form:

$$\text{div} \varepsilon \vec{E} = \rho, \quad (1)$$

with the continuity equation in complex form:

$$\text{div} \vec{J} = -j\omega\rho, \quad (2)$$

where  $\vec{E}$  is the electric field,  $\rho$  is the volume charge density,  $\vec{J}$  is the current density and  $\omega$  is the angular frequency.

Making use of Ohm's law,  $\vec{J} = \sigma \vec{E}$ , leads to the expression:

$$\text{div}(\sigma + j\omega\varepsilon)\text{grad}\varphi = 0. \quad (3)$$

The differential equation for the potential (3) in rectangle coordinates is given by the expression:

$$\begin{aligned} (\sigma_T + j\omega\varepsilon_T) \frac{\partial^2 \varphi}{\partial x^2} + (\sigma_T + j\omega\varepsilon_T) \frac{\partial^2 \varphi}{\partial y^2} + \\ + (\sigma_L + j\omega\varepsilon_L) \frac{\partial^2 \varphi}{\partial z^2} = 0 \end{aligned} \quad (4)$$

According to FDM, the partial derivatives of second order in equation (4) are replaced by their finite difference equivalents, which results in a system of linear algebraic equations:

$$\begin{aligned} u_{i,j,k} = \frac{1}{4 + 2S} (u_{i+1,j,k} + u_{i-1,j,k} + u_{i,j+1,k} + \\ + u_{i,j-1,k} + S \cdot u_{i,j,k+1} + S \cdot u_{i,j,k-1}) \end{aligned} \quad (5)$$

The solution of the system (5) is obtained by implementing the method of iterations [8]:

$$\begin{aligned} u_{i,j,k}^{(p+1)} = \frac{1}{4} [u_{i+1,j,k}^{(p)} + u_{i-1,j,k}^{(p)} + u_{i,j+1,k}^{(p)} + \\ + u_{i,j-1,k}^{(p)} + u_{i,j,k+1}^{(p)} + u_{i,j,k-1}^{(p)}], \quad (p=0,1,2,\dots) \end{aligned} \quad (6)$$

where the parameter  $S$  equals:

$$S = \frac{\sigma_L + j\omega\varepsilon_L}{\sigma_T + j\omega\varepsilon_T}. \quad (7)$$

The initial approximations of the potential,  $u_{i,j,k}^{(0)}$ , are obtained by implementing border conditions:

- Neumann's condition on the side and upper surfaces  $\left(\frac{\partial \varphi}{\partial n} = 0\right)$ ; (8)
- zero potential on the bottom surface.

However, in this demanding case, the values for the potential near a point current source tend to infinity. In order to avoid the complications induced by that tendency, analytically obtained values are used for the source's neighbouring nodes.

#### IV. VERIFICATION OF THE NUMERICAL TECHNIQUE

The numerical procedure is verified by analyzing a case of a grounded imperfect conductor layer with unlimited dimensions in the direction of the  $x$  and  $z$  axis, located in air [9]. The analytical solution for the potential in that case is used for verification of the values obtained by the numerical procedure.

##### A. Analytical solution for a layer of muscle tissue

The analytical solution of a system consisted of a layer of grounded imperfect conductor with unlimited dimensions in the direction of the  $x$  and  $z$  axis, located in air, is based on the image series theory [10]. Firstly, by solving the differential equation (4), a solution is obtained for the potential originating from a single point current source placed in an infinite environment with the characteristics of muscle tissue:

$$\varphi = \frac{I}{4\pi\sqrt{(\sigma_T + j\omega\varepsilon_T)(\sigma_L + j\omega\varepsilon_L)}\sqrt{x^2 + y^2 + k^2z^2}} \quad (9)$$

Applying the image series theory leads to the superposition expression for the potential:

$$\begin{aligned} \varphi = & \frac{-I}{4\pi\sqrt{(\sigma_T + j\omega\varepsilon_T)(\sigma_L + j\omega\varepsilon_L)}} \left[ \frac{1}{\sqrt{x^2 + y^2 + k^2z^2}} - \right. \\ & - \frac{1}{\sqrt{x^2 + (2L - y)^2 + k^2z^2}} - \frac{1}{\sqrt{x^2 + (2L + y)^2 + k^2z^2}} + \\ & + \frac{1}{\sqrt{x^2 + (4L - y)^2 + k^2z^2}} + \frac{1}{\sqrt{x^2 + (4L + y)^2 + k^2z^2}} - [0,1] \\ & \left. - \frac{1}{\sqrt{x^2 + (6L - y)^2 + k^2z^2}} - \frac{1}{\sqrt{x^2 + (6L + y)^2 + k^2z^2}} + \dots \right] \quad (10) \end{aligned}$$

During the superposition process the change introduced by every image potential member to the calculated values for the potential sum is controlled. When the point is reached at which further addition leads to no significant change in the sum (for example, less than 1.5%), the superposition process can be ended.

##### B. Numerical solution for a layer of muscle tissue

In order to examine the  $x$  and  $z$  dimensions of the layer which allow it to be considered as approximately infinite, a series of control calculations were performed. The resultant lengths of  $L_x = 400$  mm and  $L_z = 600$  mm were obtained when the point was reached, at which further increasing of  $L_x$  and  $L_z$  lead to no significant change (it was chosen, for example, less than 1.5%) in the previously calculated values for the potential.

##### C. Comparison of results

The compared numerical and analytical results along the line  $y = 0, z = 0$ , for the layer case ( $N_y = 50, N_x = 200, N_z = 300$ ), used for verification of the developed numerical method's accuracy, are presented in table 1:

TABLE 1: ANALYTICALLY AND NUMERICALLY OBTAINED VALUES FOR THE POTENTIAL ALONG THE LINE  $y = 0, z = 0$ .

$r_x$ [mm]	$\varphi_x^A$ [V]	$\varphi_x$ [V]
10	7.8412	7.8151
20	3.6418	3.5939
30	2.2434	2.2006
40	1.5474	1.5091
50	1.1334	1.0986
60	0.8612	0.8292
70	0.6705	0.6408
80	0.5306	0.5032
90	0.4255	0.3997
100	0.3590	0.3202

The maximum value of the relative error obtained by multiple control calculations and comparisons of analytical and numerical results approaches 3 %. Considering that the method was applied on a simple model whose resolution was chosen by compromise between precision and time consumption, it can be concluded that the results obtained by the developed method are of high precision.

#### V. RESULTS

The distribution of the electric potential calculated on the cross-section  $y = 0$  at  $f = 0$  Hz are presented in Fig. 4.

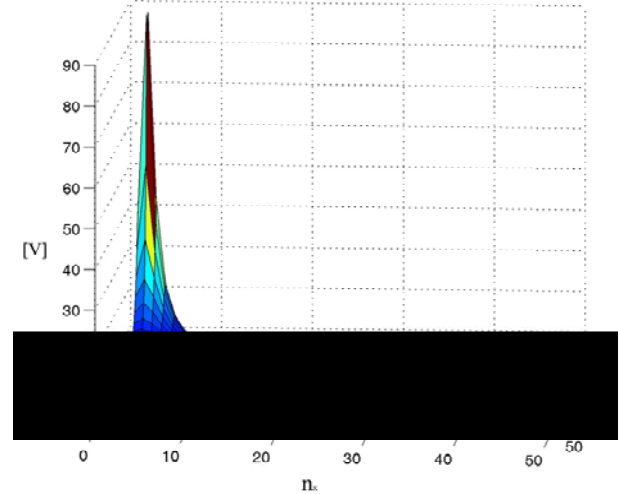


Fig 4: Potential distribution on the cross section  $y = 0$ .

The model symmetry allows partial presentation of the potential, i.e. one half of the cross section. As shown in Fig. 4, the maximum value of the potential is approximately 90 V, and appears in the vicinity of the current source which is located in the origin. It is visible on Fig. 4 that the potential function rapidly approaches 0 V, relatively near the current source. Because of the fact that the potential value equals 0 V in the remaining area of the cross-section, only the interesting part of it is shown on Fig. 4.

For comparison, the distribution of the potential determined in [11] is presented in Fig. 5.

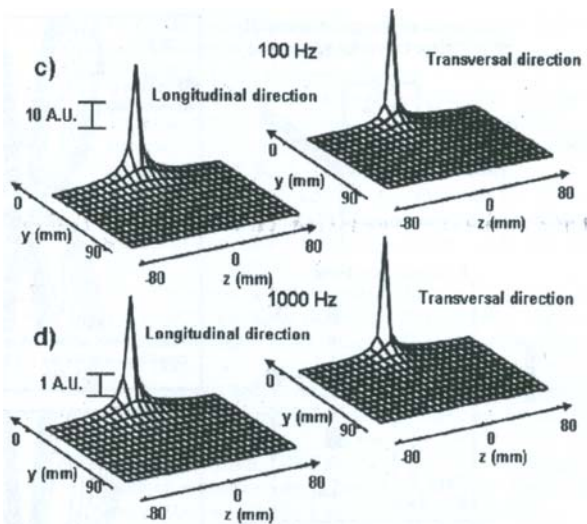


Fig. 5: Potential distribution in a system of a grounded conducting layer with unlimited dimensions in the direction of the  $x$  and  $z$  axis, according to [11].

Using the determined values for the electric potential in frequency domain, the values for the current density components ( $\vec{J} = \sigma \vec{E}$ ), at every frequency are calculated by approximating the first derivation of the potential with the following finite differences relations:

$$\left(\frac{\partial u}{\partial x}\right)_{ij} \approx \frac{u_{i+1,j} - u_{i-1,j}}{2h_x}, \quad \left(\frac{\partial u}{\partial y}\right)_{ij} \approx \frac{u_{i,j+1} - u_{i,j-1}}{2h_y}. \quad (11)$$

In order to illustrate the performance of the developed technique, the current pulse shape is determined in different locations of the muscle model. Fig. 6 shows the total current shape in 3 different points located on 30, 40 and 50 mm distance from the current source in the direction of the  $z$  axis.

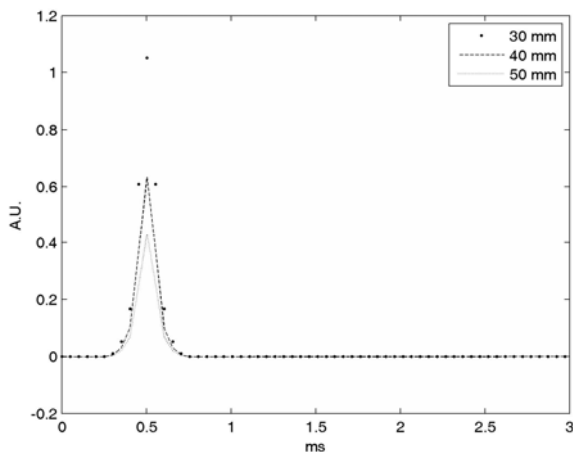


Fig. 6: Total current density calculated in 3 locations (at 30, 40 and 50 mm distance from the current source).

The values of the capacitive component of the current density calculated in 3 locations are presented in Fig. 7.

The current pulse amplitude is expected to decrease when the distance from the current source is increased. That expected tendency can be noticed on Fig. 6 and Fig. 7, for the distances 30, 40 and 50 mm from the current source.

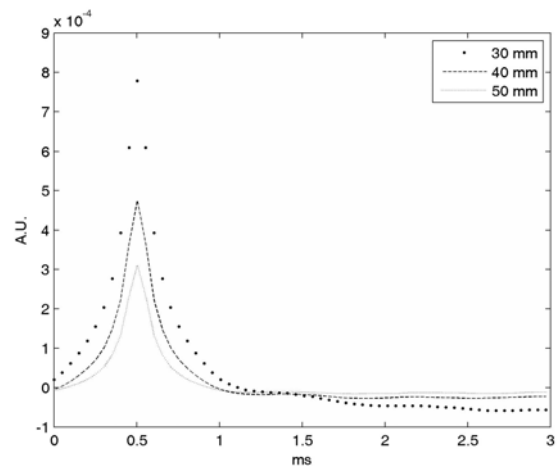


Fig. 7: Capacitive component of the current density calculated in 3 locations (at 30, 40 and 50 mm distance from the current source).

## VI. CONCLUSIONS

The presented method determines the electric potential distribution in a human muscle excited by a pulse source, taking into account the anisotropic and dispersive properties of the muscle tissue. The obtained results show the influence of the properties on the current distribution. The developed method can be used for determination of current for muscle model consisted of several different tissues. The application of the method can be extended for optimization of electrode shape.

## REFERENCES

- [1] V. Krasteva and S. Papazov "Estimation of Current Density Distribution under Circular Electrodes for External Defibrillation" *Biomedical Engineering OnLine*, Dec. 2002;
- [2] J. D. Wiley and J. G. Webster "Analysis and Control of the Current Distribution under Circular Dispersive Electrodes" *IEEE Trans. on Biomedical Engineering*, vol. BME-29, No. 5, pp. 381-389, May 1982;
- [3] A. M. Sagi-Dolev, D. Prutchi and R. H. Nathan "Three-dimensional Current Density Distribution Under Surface Stimulation Electrodes" *Medical & Biological Engineering & Computing*, 33, pp. 403-408, May 1995;
- [4] M. M. Lowery, N. S. Stoykov, A. Taflove and T. A. Kuiken "A Multiple-Layer Finite-Element Model of the Surface EMG Signal" *IEEE Trans. on Biomedical Engineering*, vol. 49, No. 5, pp. 446-454, May 2002;
- [5] L. M. Livshitz, P. D. Einziger and J. Mizrahi "Current Distribution in Skeletal Muscle Activated by Functional Electrical Stimulation: Image-Series Formulation and Isometric Recruitment Curve", *Annals of Biomedical Engineering*, Vol. 28, pp. 1218-1228, 2000;
- [6] R. Butikofer and P. D. Lawrence "Electrocutaneous Nerve Stimulation - I: Model and Experiment" *IEEE Trans. on Biomedical Engineering*, vol. BME-25, No. 6, pp. 526-531, Nov. 1978;
- [7] Institute for Applied Physics IFAC, "Nello Carrara", "Calculation of the Dielectric Properties of Body Tissues in the frequency range 10 Hz - 100 GHz", Italian national research council, Florence, 2007;
- [8] N. V. Kopchenova and I. A. Maron, *Computational Mathematics*, Mir Publishers, Moscow, 1975;
- [9] A. Kuhar, L. Ololoska and L. Janev: "Determining the current density distribution in human muscle tissue excited by a pulse source", *COMPUTATIONAL METHODS IN APPLIED MATHEMATICS*, CMAM-4, Bedlewo, Poland, 2010;
- [10] M. N. O. Sadiku: "Elements of Electromagnetics", 2<sup>nd</sup> Ed., Saunders College Publishing, 1994;
- [11] L. Mesin and R. Merletti "Distribution of Electrical Stimulation Current in a Planar Multilayer Anisotropic Tissue" *IEEE Trans. on Biomedical Engineering*, vol. 55, No. 2, pp. 660-670, Feb. 2008.